Journal of Sound and Vibration (1999) **223**(2), 213–230
Article No. jsvi.1998.2081, available online at http://www.idealibrary.com on IDEAL®

EVALUATION OF SCATTERED WAVE AND STRESS CONCENTRATION FIELD IN A DAMAGED SOLDER JOINT

P. DINEVA
Institute of Mechanics, Bulgarian Academy of Sciences, 1113 Sofia, Bulgaria

D. GROSS
Institute of Mechanics, TH Darmstadt, 64289 Darmstadt, Germany

AND

T. RANGELOV
Institute of Mathematics and Informatics, Bulgarian Academy of Sciences, 1113 Sofia, Bulgaria

(*Received* 29 *April* 1998, *and in final form* 13 *October* 1998)

Two different, but equally important problems for solder joint reliability are solved. The evaluation of the dynamic stress concentration field in the thin base layer of a damaged solder joint is the first one. It is considered as a rectangular plate with a central macro-crack surrounded with randomly distributed micro-cracks, subjected to uniform time–harmonic tension. The damaged solder joint state is described by the model of Gross and Zhang [1] (*International Journal of Solids and Structures* **29**, 1763–1779). The information of the stress concentration field in a damaged solder joint is important to understand the mechanisms in the base components of all electronic packages.

The second problem is ultrasonic wave scattering in a solder joint damaged by micro-cracks, considered as a two-dimensional finite multi-layered system. The solution of this problem may aid the creation of the modern non-destructive evaluation method (NDEM) for a high quality control of products in electronic industry.

The method of the solution of both boundary-value problems is a direct BIEM (boundary integral equation method). The numerical results obtained for a solder joint with real geometry and physical properties show how the acoustic and stress concentration fields depend on the solder joint damage state. The character of this dependence is discussed.

© 1999 Academic Press

1. INTRODUCTION

Solder systems for the electronics industry now offer a unique technological opportunity. As the electronics industry moves in the direction of miniaturization, the use of surface mount components (SMC) increases. As a result, the reliability of SMCs becomes a critical issue. The solder joint is the

0022–460X/99/220213 + 18 $30.00/0
© 1999 Academic Press

only mechanical means of attaching the SMC to the printed circuit board (PCB) and provides electrical and thermal continuity. The major cause of failure is low cycle thermal fatigue of the solder joints due to the fact that there is a mismatch of the coefficient of thermal expansion of the printed circuit board, solder and chip carrier. There is, however, high cycle fatigue caused by the equipment vibration too. SMCs utilized in avionics and naval marine applications are subjected to high frequency vibrations. High quality product requirements in the electronics industry concern directly the solder joint reliability problem and the study of both the dynamic stress-concentration field and scattering of ultrasonic waves in a damaged solder joint.

High quality product requirements in the electronics industry involve high quality control in their manufacturing. The information for solder microstructure at various damage states can be obtained by non-destructive methods. These methods need precise and adequate mechanical models for ultrasonic wave propagation in cracked solder joints.

Two base phenomena, the wave attenuation and the dispersion, are the sources of huge information about the damaged state of the material. Most studies on wave attenuation and dispersion, see references [2–6], are in the frame of Rayleigh regime, where the wavelength is much larger than the crack's dimensions. Some others are in the frame of the diffusive regime for the opposite case. Few studies consider the stochastic regime, where the wavelength and the characteristic dimensions are of the same order. A detailed analysis of the previous investigations on the wave attenuation and dispersion in damaged solids is performed in reference [7]. This paper uses the damaged model of Gross and Zhang [1], which gives the procedure for calculating the attenuation coefficient and the phase velocity of waves propagating in a damaged solid containing a distribution of completely randomly oriented micro-cracks. The essential advantage of this approach is that it puts no limitation on frequency and requires only a few parameters describing the statistical distribution and orientation of the micro-cracks.

To represent a solder joint with real geometrical and mechanical properties as a place of multiple scattering and stress concentration is the aim of the paper. So, the following elasto-dynamic problems are solved: stress intensity factor (SIF) calculation of the centrally cracked solder joint's thin base Cu-layer considered as a centrally cracked rectangular plate subjected to uniform time-harmonic tension in both cases: one central macro-crack without and with surroundings of micro-cracks described in reference [1]; ultrasonic (time-harmonic) wave propagation in a finite multi-layered system: PCB–thin Cu layer–solder joint, the damaged state of which is described by the model in reference [1].

The BIEM is used for the solution of the two-dimensional time-harmonic boundary-value problems. The accuracy of the solution method is checked by comparing the results obtained for the dynamic behavior of a centrally cracked rectangular plate with those in reference [8].

The rest of the paper is organized as follows. Section 2 considers the model in reference [1] for wave propagation in damaged solids. Section 3 presents the

formulation, solution and numerical results of the problem of SIF calculation of the centrally cracked solder joint's base layer. Section 4 shows the formulation, solution and numerical results for ultrasonic wave propagation in a solder joint damaged by randomly distributed slit micro-cracks. Conclusions are given in section 5.

2. DESCRIPTION OF THE DAMAGE STATE MODEL

The model of Gross and Zhang [1] is used to describe the dispersion of elastic waves in a solid permeated by a random distribution of micro-cracks. Its main features and its advisability for a solution of the above-defined solder joint problems will be discussed. The model base assumptions are: the solid is homogeneous, isotropic and linear elastic and contains distributed micro-cracks; the location and orientation of micro-cracks is random; geometrical and dynamical interactions amongst individual cracks are neglected, i.e., the model is suitable for small crack densities; the crack-faces are not in touch and the traction-free boundary condition is satisfied; all cracks are identical with the same geometrical dimension. The existing experimental data, see references [9–12], for a solder joint microstructure shows that the above assumptions are acceptable for the description of the solder joint damage state.

The effective medium approach is used. The original, inhomogeneous and cracked solid is presented by a statistically homogeneous solid with macroscopic isotropy, which has the same overall average response. The effective medium of the cracked solid still remains linear, causal and passive as in its originally uncracked state. The material is homogenized by a representative volume, large enough compared to the dimensions of the micro-cracks and small enough compared to body dimensions. In analogy to visco-elastic wave propagation in a homogeneous material, the overall average dynamic response can be described by a complex and frequency dependent wave number

$$K(\omega) = \frac{\omega}{\bar{C}(\omega)} + \mathrm{i}\alpha(\omega), \tag{1}$$

where $\bar{C}(\omega)$ is the effective wave velocity and $\alpha(\omega)$ is the attenuation coefficient. Under the assumptions of neglecting crack interactions, the equation of Foldy [13] allows one to obtain the wave number of the cracked solid from the wave number of the uncracked solid, the forward scattering amplitude (calculating numerically by BIEM) and the number n of cracks per unit area. $\bar{C}(\omega)$ and $\alpha(\omega)$ can be determined from the real and imaginary parts of $K(\omega)$.

In the casual approach used in reference [1], the solution procedure consists of three steps. The scattering cross section of a single crack is calculated numerically by the BIEM. The scattering cross-section γ describes the effect of the crack on the energy withdrawal from the incident wave

$$\gamma = \frac{\langle P^{sc} \rangle}{\langle I \rangle},$$

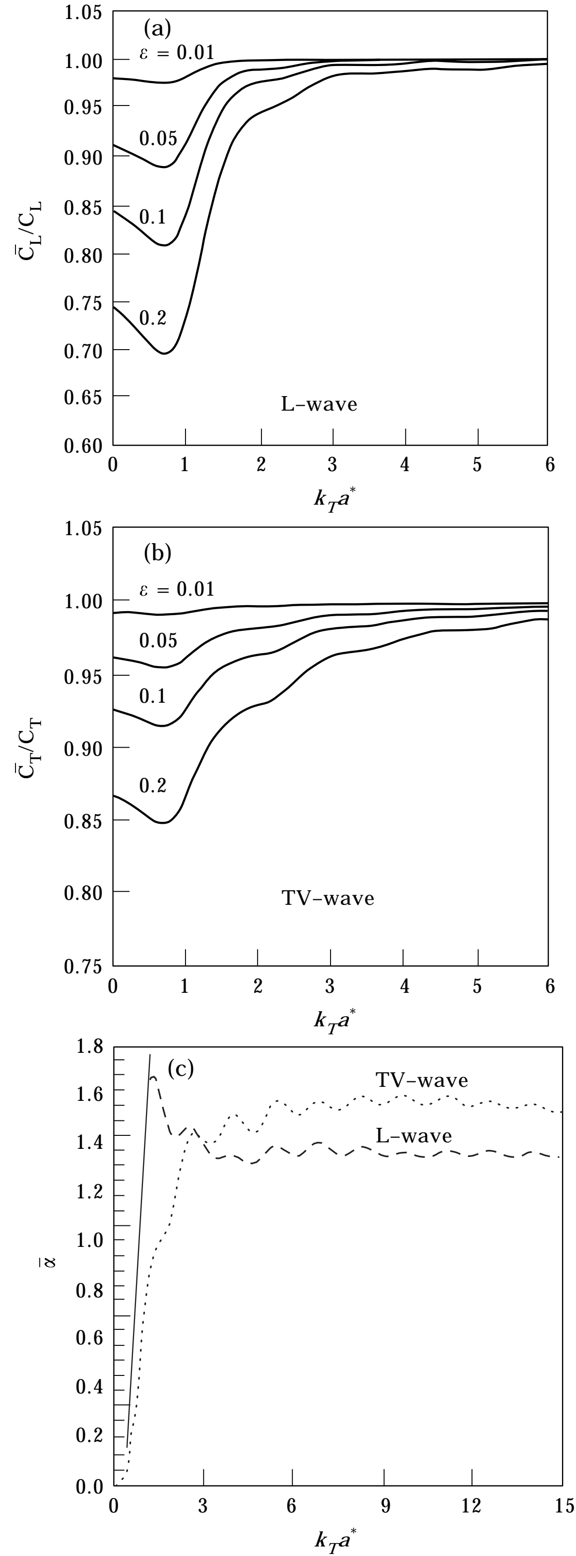

Figure 1. (a, b) Normalized effective wave velocity by the Zhang and Gross model [14] versus $k_T a^*$. (c) Normalized attenuation coefficient by the Zhang and Gross model [14] versus $k_T a^*$. Reprinted from reference [14], copyright (1993), with permission from Elsevier Science.

where $\langle P^{sc} \rangle$ denotes the time-average power flow of scattered waves, and $\langle I \rangle$ represents the time averaged intensity of the incident wave. Then, the attenuation coefficient, using simple energy consideration, is expressed by

$$\alpha = \frac{1}{2} n \gamma.$$

Since the solid is a linear, causal and passive system, the real and the imaginary part of the complex effective wave number are not independent of each other. The effective wave velocity is computed by the Kramers–Kroning relations. The effective elastic characteristics can be obtained for the effective medium of a cracked solid. For the aim of the present work, the authors used the results in references [1, 7, 14] for the case of randomly oriented slit cracks but under assumption for small attenuation coefficient. Figures 1(a) to (c) are taken from reference [14], where $k_T a^*$ is a dimensionless wave number, $k_T = \omega / C_T$ and a^* is half micro-crack length, C_T is the shear wave velocity of the uncracked solid; ε is the universal crack-density parameter, introduced in reference [15], $\varepsilon = (4/\pi) n a^{*2}$ for the material damaged by slit cracks. Both parameters n and a^* defining the crack-density parameter ε, can be obtained experimentally by QNDE measurements. The normalized attenuation coefficient $\bar{\alpha}$ versus $k_T a^*$ is shown in Figure 1(c), where

$$\bar{\alpha} = \frac{4a^*}{\pi \varepsilon} \alpha.$$

It can be seen from Figure 1(a) to (c) that when the dimensionless wave number $k_T a^*$ belongs to the interval (0·0, 0·5] then the normalized attenuation coefficient $\bar{\alpha}$ belongs to the interval (0·0, 0·05], the normalized effective wave velocity $\bar{C}_L / C_L$ belongs to the interval [0·745, 0·69] at $\varepsilon = 0{\cdot}2$ and the normalized effective wave velocity $\bar{C}_T / C_T$ belongs to the interval [0·865, 0·845] at $\varepsilon = 0{\cdot}2$. Thus at the mentioned frequency interval (0·0, 0·5] the imaginary part $\alpha(\omega)$ of the complex wave number $K(\omega)$ at (1) is negligibly small compared with its real part $\omega / \bar{C}(\omega)$. The solution and the numerical results in sections 3 and 4 are obtained in such a frequency interval providing the negligible small attenuation coefficient.

3. SOLDER JOINT AS A PLACE OF DYNAMIC STRESS CONCENTRATION

Here a hybrid model is presented by using both the model of Gross and Zhang [1] for finding effective wave velocities in a field with micro-cracks and the displacement BIEM for the solution of a two-dimensional problem for a centrally cracked rectangular plate under uniform time-harmonic tension.

3.1. THE BOUNDARY-VALUE PROBLEM

The solder joint is presented as a scheme in Figure 2(a). The solder joint system is presented as a finite three-layered body consisting of printed circuit

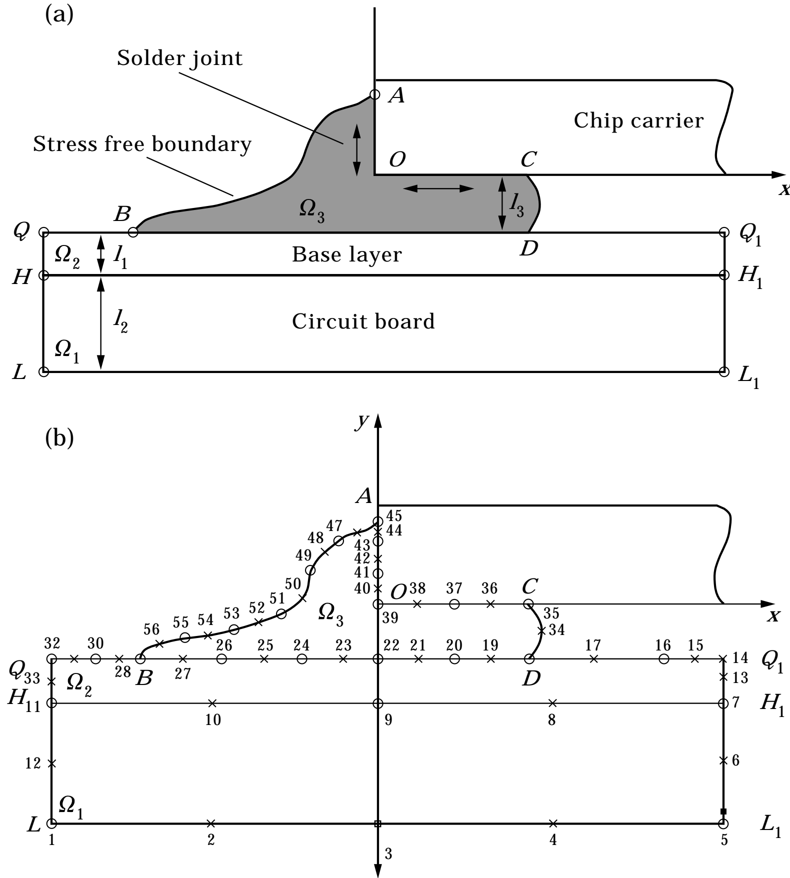

Figure 2. (a) Solder joint cross-section geometry (problem 2). (b) The BE-mesh (problem 2).

board—Ω_1 range, thin base Cu-layer—Ω_2 range and solder—Ω_3 range. In this section only the base Cu-layer (Ω_2 layer) as a centrally cracked rectangular plate subjected to time-harmonic uniform tension on its horizontal boundaries will be considered. The following assumptions are made: due to the symmetry a quarter of the center-cracked plate can be considered and the geometry of the problem is shown in Figure 3(a); a plane-strain state is considered and the displacement has two components $\mathbf{u} = (u_x, u_y)$.

The governing equations are:

$$\sigma_{ij,j} + \rho\omega^2 u_i = 0, \tag{2}$$

where ρ is density, ω is frequency, σ_{ij} and u_i are stress and displacement, respectively.

The boundary conditions are given in Figure 3(a). If the material is damaged by randomly distributed micro-cracks, the wave velocity is calculated using the

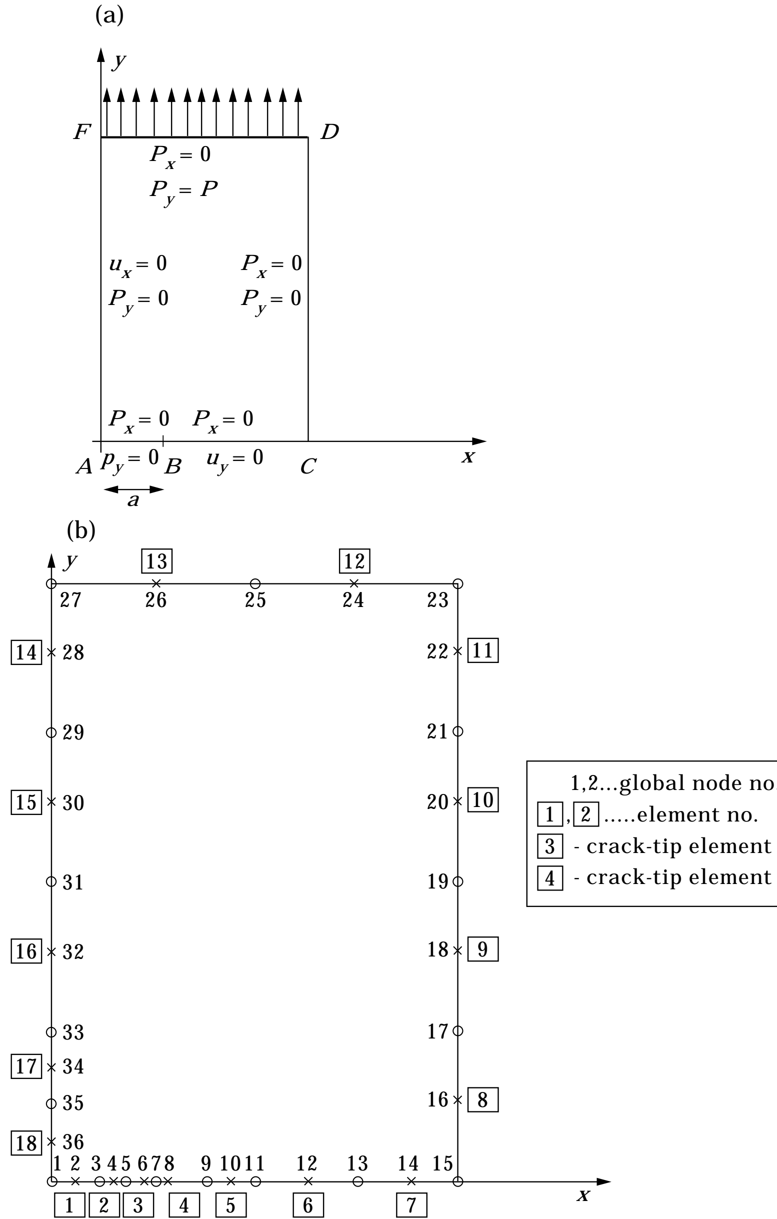

Figure 3. (a) A quarter of the center cracked plate (problem 1). (b) The BE-mesh (problem 1).

Gross and Zhang model [1] and the effective wave numbers for TV-waves and L-waves are

$$k_T^* = \frac{\omega}{\bar{C}_T}; \quad k_L^* = \frac{\omega}{\bar{C}_L}.$$

3.2. DIRECT BIE FORMULATION OF THE PROBLEM

The governing BIEs are:

$$c_{ij}u_j(\mathbf{r},\omega)=\int_{ABCDFA}U^*_{ij}(\mathbf{r},\mathbf{r}_0,\omega)p_j(\mathbf{r}_0,\omega)\,\mathrm{d}\Gamma-\int_{ABCDFA}P^*_{ij}(\mathbf{r},\mathbf{r}_0,\omega)u_j(\mathbf{r}_0,\omega)\,\mathrm{d}\Gamma. \tag{3}$$

Here U^*_{ij}, P^*_{ij} are the displacement and the traction fundamental solutions of equation (2) (see Appendix), $c_{ij}=\delta_{ij}/2$ on the smooth boundary; $\mathbf{r}$, $\mathbf{r}_0$ are position vectors of the field and the source point; $\mathbf{u}$, $\mathbf{p}$ are unknown displacement and traction vectors. The boundary integral equation (3) together with boundary conditions describe the boundary-value problem to be solved by the displacement BIEM. The boundary discretization is made according to the following rules: the length of the elements is $\Delta l\leqslant\lambda_T/10$, where λ_T is the length of the TV-wave (see Figure 3(b)). Here the quarter point boundary element is adopted to compute the dynamic SIF, and the following condition is satisfied

$$0{\cdot}05\leqslant\frac{L^*}{a}\leqslant 0{\cdot}25,$$

where L^* is the length of the crack-tip element, a is the half macro-crack length. Displacement and traction at arbitrary points between the nodes are expressed in terms of nodal values u^e_j, p^e_j using finite element shape functions:

$$p(\xi)=\sum_1^3 N_j(\xi)p^e_j,\quad u(\xi)=\sum_1^3 N_j(\xi)u^e_j.$$

The parabolic elements are used

$$N_1=\frac{\xi(\xi-1)}{2},\quad N_2=1-\xi^2,\quad N_3=\frac{\xi(\xi+1)}{2}.$$

An intrinsic co-ordinate ξ is designed for each triplet of nodal points, taking values -1, 0, $+1$ at the first, middle and third nodes respectively. (x^p, y^p) is the field point, (x^q_1, y^q_1), (x^q_3, y^q_3) are the first and third point of the corresponding BE and $r_{x,1}=x^q_1-x^p$, $r_{y,1}=y^q_1-y^p$, $r_{x,3}=x^q_3-x^p$, $r_{y,3}=y^q_3-y^p$. The required co-ordinates of the Gaussian quadrature used: for ordinary quadratic BE

$$r_i(\xi)=r_{i,1}+\left(\frac{\xi+1}{2}\right)(r_{i,3}-r_{i,1}),\text{ with the Jacobian } J=\frac{l}{2};$$

for the left crack-tip BE

$$r_i^{left}(\xi)=r_{i,1}+\left(\frac{\xi+1}{2}\right)^2(r_{i,3}-r_{i,1}),\text{ with the Jacobian } J=\frac{\xi+1}{2}l;$$

for the right crack-tip BE

$$r_i^{right}(\xi) = r_{i,3} + \left(\frac{\xi - 1}{2}\right)^2 (r_{i,1} - r_{i,3}), \text{ with the Jacobian } J = \frac{1 - \xi}{2} l,$$

where l is the BE length.

After boundary discretisation the system of integral equations is written for a number of discrete points, which are the nodal points of BE. An algebraic system according to the unknowns of the mixed boundary-value problem is obtained after boundary condition satisfaction and solution of singular and non-singular integrals.

The SIF calculation is made using the formulae, see reference [16].

$$K_l = \frac{\mu}{2(1 - \nu)} \sqrt{\frac{2\pi}{l}} (4u_{yB} - u_{yC}),$$

where μ, ν are shear modulus and Poisson ratio and u_{yB}, u_{yC} are the displacements near the crack-tip.

3.3. NUMERICAL RESULTS

The mechanical and geometrical parameters of the problem considered are density $\rho = 0{\cdot}896 \times 10^{-5}$ kg/mm^3; Lame constant $\lambda = 0{\cdot}707 \times 10^6$ N/mm^2, Poisson ratio $\nu = 0{\cdot}2976$, shear modulus $\mu = 0{\cdot}4810 \times 10^5$ N/mm^2, $AC = 2{\cdot}0$ mm, $CD = 0{\cdot}5$ mm. The value of the amplitude of the time-harmonic traction is $\sigma = 20$ N/mm^2 and the macro-crack size is $2a = 1$ mm.

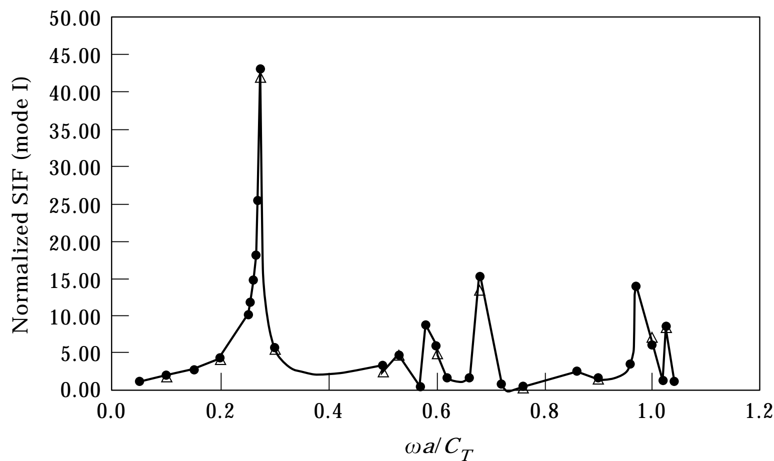

Figure 4. Normalized SIF for a center cracked plate under uniform time-harmonic tension. ●, Authors' results; ▲, Chirino and Dominguez [8].

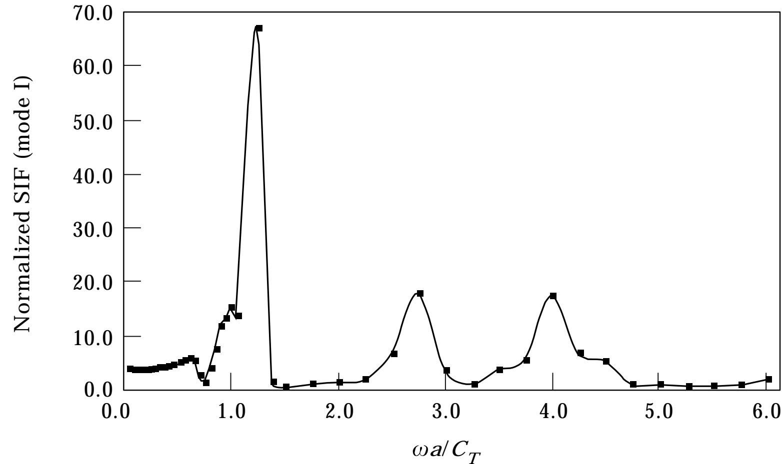

Figure 5. Normalized SIF for a solder joint Cu-layer under uniform time-harmonic tension in the case when there is one central macro-crack and the rest of material is undamaged.

The used boundary element mesh is given in Figure 3(b). The number of the boundary elements along the half crack *AB* is 3, along the boundary *BC* is 4, along the boundary *CD* is 4, along the boundary *DF* is 2, along the boundary *FA* is 5.

The test example for dynamic behavior of a centrally cracked rectangular plate under uniform time harmonic tension is solved and results are compared with those in reference [8] (see Figure 4). The good agreement between the results confirms that the problem has been solved accurately.

The magnitude of the mode I dynamic SIF normalized by $\sigma\sqrt{\pi a}$ for centrally cracked solder joint base Cu-layer in the case where there is not a field of micro-cracks is shown versus frequency in Figure 5. The same curve is shown in Figures 6 and 7 in the cases when there is an environment of randomly distributed slit micro-cracks with size $a^* = a/10$ at different values of crack-density parameter ε. The data for effective wave velocity are taken from Figures 1(a) and (b).

The computed dynamic SIF shows clear that: more oscillatory behavior in the case of distributed micro-cracks occurs; the static value is exceeded, which is specially important for small objects such as solder joints; the existence of micro-cracks changes the character of the frequency dependence of the normalized mode I dynamic SIF—the largest maximum values occur at higher frequencies; a considerable decrease of the value of normalized SIF occurs in the case of the effective medium of micro-cracks.

The calculation of SIF in the cases of a macro-crack in the plate damaged by randomly distributed slit micro-cracks throws light on the evaluation of the dynamic stress-concentration field in solder joints.

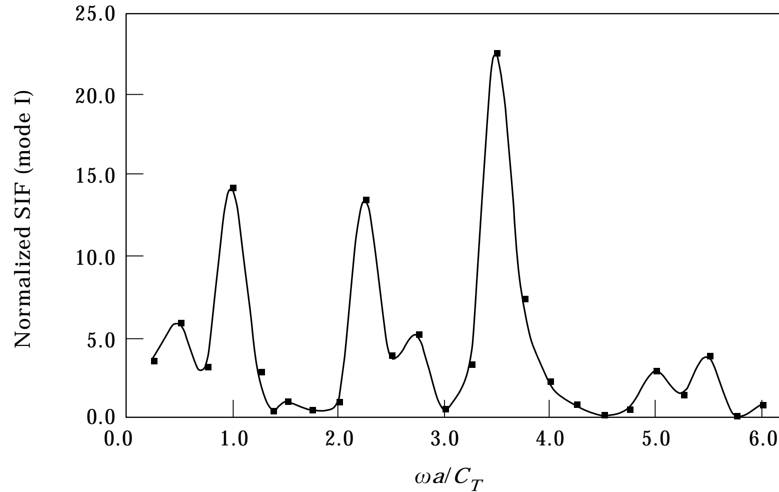

Figure 6. Normalized SIF for a solder joint Cu-layer in the case when there is one central macro-crack and the rest of material is damaged by randomly distributed slit micro-cracks at $\varepsilon = 0{\cdot}1$.

4. ULTRASONIC WAVE PROPAGATION IN A DAMAGED SOLDER JOINT

4.1. THE BOUNDARY-VALUE PROBLEM

The solder joint is considered as a finite three-layered body. Let us denote its cross-section in the (x, y) plane as $\Omega = \Omega_1 \cup \Omega_2 \cup \Omega_3$, where Ω_i, $i = 1, 2, 3$ are the cross-sections of the layers $\Omega = \Omega_1 \cup \Omega_2 \cup \Omega_3$ (see Figure 2(a)). The range Ω_1 is the printed circuit board with boundary $\Gamma_{\Omega_1} = LL_1 \cup L_1H_1 \cup H_1H \cup HL$. The

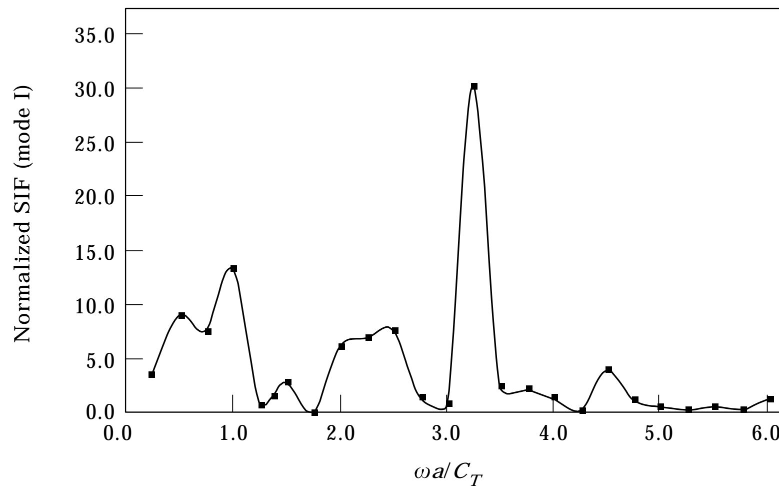

Figure 7. Normalized SIF for a solder joint Cu-layer in the case when there is one central macro-crack and the rest of material is damaged by randomly distributed slit micro-cracks at $\varepsilon = 0{\cdot}2$. Reprinted from *Int. J. of Engineering Science*, **31,** 6. Zhang & Gross: “Wave attenuation and dispersion . . . . ”, pp. 841–858. Copyright (1993), with permission from Elsevier Science.

TABLE 1

Physical constants

Number of range	Material	Density (kg/mm^3)	Lame constant (N/mm^2)	Poisson constant	Shear module (N/mm^2)	Wave shear velocity (mm/s)	Wave longitudinal velocity (mm/s)
Ω_1: circuit board	Laminated insulation	$0{\cdot}106000 \times 10^{-5}$	$0{\cdot}740840 \times 10^{4}$	0·4000	$0{\cdot}2450 \times 10^{4}$	$0{\cdot}15200 \times 10^{7}$	$0{\cdot}29110 \times 10^{7}$
Ω_2: base layer	Cu	$0{\cdot}896000 \times 10^{-5}$	$0{\cdot}70702 \times 10^{5}$	0·2976	$0{\cdot}4810 \times 10^{5}$	$0{\cdot}23170 \times 10^{7}$	$0{\cdot}43160 \times 10^{7}$
Ω_3: solder joint	Pb	$0{\cdot}114000 \times 10^{-4}$	$0{\cdot}42007 \times 10^{5}$	0·4413	$0{\cdot}5590 \times 10^{4}$	$0{\cdot}0700250 \times 10^{7}$	$0{\cdot}21600 \times 10^{7}$

TABLE 2

Geometrical parameters

Boundary	Length (mm)
LL_1	4·0
HH_1	4·0
QQ_1	4·0
OA	1·0
CO	0·8
BQ	0·8
DB	2·0
Q_1B	1·2
DC	0·1
H_1Q_1	0·1
QH	0·1
L_1H_1	1·5
HL	1·5

range Ω_2 is the thin base layer with boundary $\Gamma_{\Omega_2} = HH_1 \cup H_1Q_1 \cup Q_1Q \cup QH$. The range Ω_3 is the solder joint with boundary $\Gamma_{\Omega_3} = BD \cup DC \cup CO \cup OA \cup AB$. The base layer Ω_2 and the solder joint Ω_3 are damaged due to the technological, service or environment conditions. The printed circuit board Ω_1 is considered as an undamaged domain. The damage state is described by the model in reference [1] and is discussed in section 2. As an incident time-harmonic wave by the L-wave generator with a frequency ω and amplitude $u_{i0}(x, y)$ impinges on the boundary LL_1 (see Figure 2(a)) of the system: PCB–base layer–solder joint, scattered waves are generated. The scattered wave field is time-harmonic too. It can be observed by the receiver amplifier and it can be obtained by the solution of the boundary–value problem for the wave amplitude $u_i(x, y, \omega)$.

The governing equation (2) for plain-strain state is considered.

The boundary conditions are:

$$
\begin{aligned}
& u_i = u_{i0} \quad \text{for} \quad (x, y) \in LL_1, \\
& \sigma^1_{ij} n_j|_{HH_1} = \sigma^2_{ij} n_j|_{HH_1}, \quad u^1_i|_{HH_1} = u^2_i|_{HH_1}, \\
& \sigma^2_{ij} n_j|_{BD} = \sigma^3_{ij} n_j|_{BD}, \quad u^2_i|_{BD} = u^3_i|_{BD}, \\
& \sigma_{ij} n_j = 0 \quad \text{for} \quad (x, y) \in AB \cup BQ \cup Q_1D \cup DC \cup QL \cup L_1Q_1, \\
& u_i = 0 \quad \text{for} \quad (x, y) \in OA \cup OC, \\
& \sigma_{ij} n_j|_{S^+_{cr}} = 0,
\end{aligned}
$$

where $\sigma^l_{ij} = \sigma_{ij}|_{\Omega_l}, u^l_i = u_i|_{\Omega_l}$, $l = 1, 2, 3$. Rigid boundary conditions on the boundaries OA and OC will represent a damaged solder, softer than chip carrier's material.

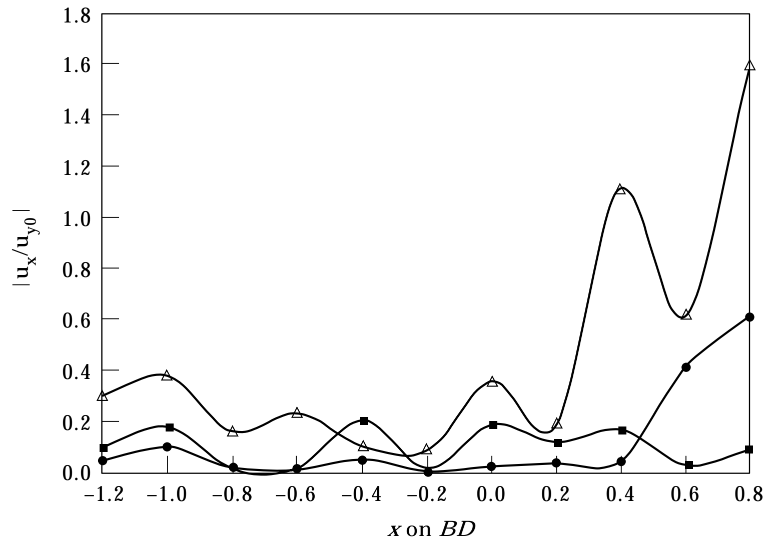

Figure 8. $|u_x/u_{y0}|$ at $k_T a = 6{\cdot}0$ on the boundary BD for damaged solder joint: ●, undamaged case; ■, damaged case with $\varepsilon = 0{\cdot}1$; ▲, damaged case with $\varepsilon = 0{\cdot}2$.

The formulated boundary-value problem is solved by BIEM, using parabolic BE.

4.2. NUMERICAL RESULTS

The scattered ultrasonic wave field in an undamaged and in a damaged solder joint is obtained numerically. Figures 1(a) and (b) from reference [14] are used for evaluation of the effective velocities of base Cu-layer and Pb solder joint damaged by randomly distributed slit micro-cracks at different crack-density

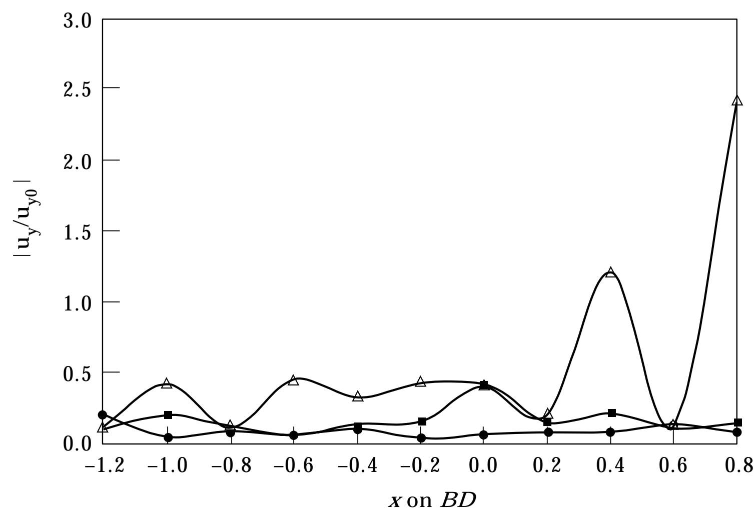

Figure 9. $|u_y/u_{y0}|$ at $k_T a = 6{\cdot}0$ on the boundary BD for damaged solder joint: ●, undamaged case; ■, damaged case with $\varepsilon = 0{\cdot}1$; ▲, damaged case with $\varepsilon = 0{\cdot}2$.

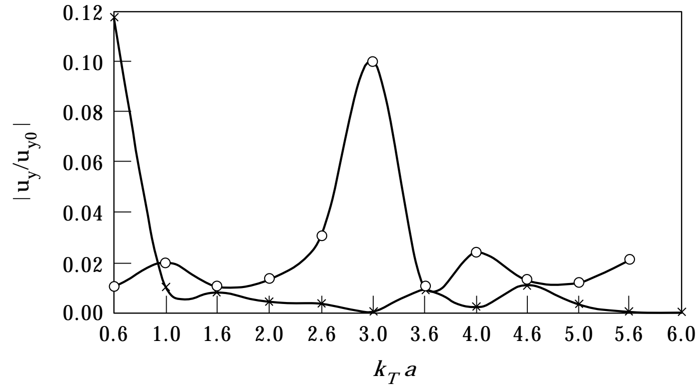

Figure 10. $|u_y/u_{y0}|$ versus $k_T a$ in point $\in HH_1(x = 0{\cdot}0)$ at: ×, undamaged solder joint; ○, damaged solder joint with $\varepsilon = 0{\cdot}05$.

parameters. Mechanical properties of the undamaged solder-joint system are shown in Table 1. Geometrical characteristics of the system considered are shown in Table 2. The incident wave amplitude is: $u_{x0} = 0{\cdot}0$, $u_{y0} = 0{\cdot}1 \times 10^{-5}$ mm. The micro-crack half-length is $a^* = 0{\cdot}01$ mm. The used boundary element mesh for the multi-layered solder joint system is given in Figure 2(b).

Parametric study of the solder joint time-harmonic response with respect to the crack-density parameter ε is shown in Figures 8 and 9. It can be seen that with the increase of the crack density parameter ε, the components of displacement in the points of boundary *BD* increase and are rather different from the undamaged case. It is obvious that the acoustic picture is sensitive to the micro-cracks existence. Boundary *BD* is selected due to the fact that in the

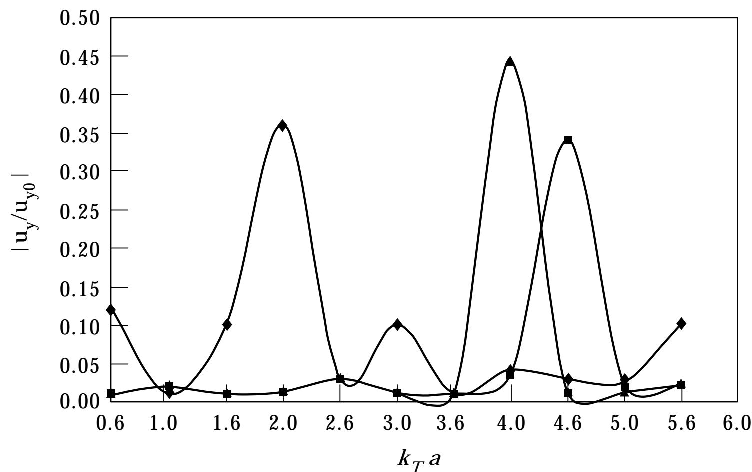

Figure 11. $|u_y/u_{y0}|$ versus $k_T a$ in point $\in HH_1(x = 0{\cdot}0)$ at: ■, damaged solder joint with $\varepsilon = 0{\cdot}2$; ▲, damaged solder joint with $\varepsilon = 0{\cdot}1$; ◆, damaged solder joint with $\varepsilon = 0{\cdot}01$.

case of the cracking processes development on this boundary the so-called "cold solder joint" is available. In this case the solder joint cannot provide any electrical connection between electronic package's components. These cases directly concern the reliability of electronic packages.

Numerical study of the solder joint time-harmonic response with respect to the frequency is shown in Figures 10 and 11 at different crack-density parameters for the case of slit micro-cracks. Here, frequency is presented via dimensionless wave number $k_T a = (\omega/C_T)\, 0{\cdot}5$. The rapid change of the frequency character of the displacement scattered field between an undamaged and a damaged solder joint, as well as between solders with different crack-density parameters can be seen.

5. CONCLUSIONS

The two-dimensional "in-plane" elasto-dynamic (time-harmonic) problem is solved by displacement BIEM for the real geometry of a damage multi-layered system: PCB–thin base layer–solder joint. The damage state is caused by a distribution of completely randomly oriented slit micro-cracks and it is evaluated by the model of Gross and Zhang [1]. Parametric study of the solder joint scattered wave field with respect to the crack-density parameter and frequency is presented.

The dynamic stress field and its concentrations in the thin Cu-layer of solder joint are studied. The solder joint base layer is considered as a centrally cracked rectangular plate subjected to uniform time-harmonic tension. The two-dimensional elasto-dynamic (time-harmonic) problem on the base of the displacement BIE formulation and quarter-point BE for the crack-tip modelling is solved. SIF is calculated for the following situations: (a) there is only one central macro-crack in the base layer and the rest of the material is undamaged; (b) there is one central macro-crack with size a but the rest of the material is damaged by randomly distributed slit micro-cracks with size $a^* \ll a$. The model of Gross and Zhang [1] of finding the effective wave velocity in a damaged solid is used.

Numerical results for SIF in the solder joint base layer in both cases are obtained and compared. The proposed model gives information about the stress concentration field in damaged solder joints.

The solution of the problem for the dynamic behavior of a centrally cracked rectangular plate under uniform time-harmonic tension by displacement BIEs and comparison of results for SIF with those obtained in reference [8] confirm that the solution is accurate. This is important, because the base geometrical element of solder joint geometry is a rectangular plate without and with a crack.

All numerical results obtained show the influence of microstructure state change on the acoustic wave picture. The dependence of the scattered wave picture and the dynamic stress-concentration field in solder joint on the crack-density parameter ε is shown in many figures.

The solution of these direct elasto-dynamic problems can be used: for an interpretation of ultrasonic QNDE experimental results; as a base of a solution

of the inverse problems for identification of solder joint microstructure characteristics; for creation of an ultrasonic NDE technique for a high quality control of the electronic components.

ACKNOWLEDGMENT

The authors acknowledge the support of the Volkswagen Foundation under the grant number I/69881.

REFERENCES

1. D. Gross and C. Zhang 1992 *International Journal of Solids and Structures* **29**, 1763–1779. Wave propagation in damaged solids.
2. D. L. Anderson, B. Minster and D. Cole 1974 *Journal of Geophysical Research* **79**, 4011–4015. The effect of oriented cracks on seismic velocities.
3. R. J. O'Conell and B. Budiansky 1974 *Journal of Geophysical Research* **79**, 5412–5426. Seismic velocities in dry and saturated cracked solids.
4. J. A. Hudson 1981 *Geophysical Journal of the Royal Astronomical Society* **64**, 133–150. Wave speeds and attenuation of elastic waves in material containing cracks.
5. M. F. McCarthy and M. H. Carroll 1984 *Wave Propagation in Homogeneous Media and Ultrasonic Nondestructive Evaluation* **62**, 141–153 New York: ASME. Wave propagation in randomly cracked media.
6. M. Piau 1980 *International Journal of Engineering Science* **18**, 549–568. Crack-induced anisontropy and scattering in stress rocs: effective elastic moduli and attenuation.
7. C. H. Zhang 1993 *Habilitationsschrift, TH-Darmstadt*. On wave propagation in cracked solids.
8. F. Chirino and J. Dominguez 1989 *Engineering Fracture Mechanics* **34**, 1051–1061. Dynamic analysis of cracks using BEM.
9. V. Raman and T. C. Reiley 1988 *Metallurgical Transactions* **19A**, 1533–1545. Cycle deformation and fracture in Pb-Su solid solution alloy.
10. L. K. Quan, D. Frear, D. Grivas and J. W. Morris 1987 *Journal of Electronic Materials* **16**, 203–208. Tensile behavior of Pb-Su solder/Cu joints.
11. G. S. Karlheinz and R. Waterschek 1984 *Welding and Cutting* **8**, E126–E128. Sound emission analysis applied to solder joints.
12. W. J. Tomlinson and G. A. Cooper 1986 *Journal of Material Science* **21**, 1730–1734. Fracture mechanism of brass/Sn-Pb-Sb solder joints and effect of production variables on the joint strength.
13. L. Foldy 1945 *Physical Review* **67**, 107–119. Multiple scattering theory of waves.
14. C. Zhang and D. Gross 1993 *International Journal of Engineering Science* **31**, 841–858. Wave attenuation and dispersion in randomly cracked solid I. Slit cracks.
15. B. Budiansky and R. O'Conell 1976 *International Journal of Solids and Structures* **12**, 81–97. Elastic moduli of a cracked solid.
16. G. E. Blandford, A. R. Ingraffea and J. A. Liggett 1981 *International Journal of Numerical Methods in Engineering* **17**, 387–404. Two-dimensional stress intensity factor computations using the boundary element method.
17. H. Bateman and A. Erdeli 1953 *Higher Transcendental Functions*. New York: McGraw-Hill.

APPENDIX

Function $U^*_{kj}(x, y, x_0, y_0, \omega)$ is the fundamental solution of the system (1), and the function $P^*_{kj}(x, y, x_0, y_0, \omega)$ is the corresponding traction.

$$U^*_{kj}(x^p - x^q, y^p - y^q, \omega) = \frac{1}{2\pi\mu}[\psi\delta_{kj} - \chi r_{,k} r_{,j}],$$

$$\begin{aligned} &P^*_{kj}(x^p - x^q, y^p - y^q, \omega); \\ &= \frac{1}{2\pi}\left\{\left(\frac{\partial\psi}{\partial r} - \frac{\chi}{r}\right)\left(\delta_{kj}\frac{\partial r}{\partial n} + r_{,k}n_j\right) - 2\frac{\chi}{r}\left(r_{,j}n_k - 2r_{,k}r_{,j}\frac{\partial r}{\partial n}\right)\right\} \\ &\quad - \frac{1}{2\pi}\left\{2\frac{\partial\chi}{\partial r}r_{,k}r_{,j}\frac{\partial r}{\partial n} - \left(\frac{C_L^2}{C_T^2} - 2\right)\left(\frac{\partial\psi}{\partial r} - \frac{\partial\chi}{\partial r} - \frac{\chi}{r}\right)r_{,j}n_k\right\}, \end{aligned}$$

where

$$r = \sqrt{(x^p - x^q)^2 + (y^p - y^q)^2}, \quad r_{,x^q} = \frac{r_x}{r} = \frac{x^q - x^p}{r}, \quad r_{,y^q} = \frac{r_y}{r} = \frac{y^q - y^p}{r},$$

(x^p, y^p) and (x^q, y^q) are the field point and the running point respectively,

$$\frac{\partial r}{\partial n} = r_{,x^q}n_{x_0} + r_{,y^q}n_{y_0}, \quad s = -\mathrm{i}\omega, \quad \chi = K_2\left(\frac{sr}{C_T}\right) - \frac{C_T^2}{C_L^2}K_2\left(\frac{sr}{C_L}\right),$$

$$\psi = \frac{1}{2}\left[K_2\left(\frac{sr}{C_T}\right) - \frac{C_T^2}{C_L^2}K_2\left(\frac{sr}{C_L}\right) + K_0\left(\frac{sr}{C_T}\right) + \frac{C_T^2}{C_L^2}K_0\left(\frac{sr}{C_L}\right)\right],$$

function $K_m(z) = -\frac{1}{2}\mathrm{i}\pi(\mathrm{i})^m \mathrm{H}_m^{(2)}(\mathrm{i}z)$ for $z = -\mathrm{i}\omega/C_T$ or $z = -\mathrm{i}\omega/C_L$ is represented with modified Bessel functions of second type, see reference [17].

The asymptotic representations of the functions U^*_{kj} and P^*_{kj} for $r \to 0$ are

$$\begin{aligned} (U^*_{kj})^{as} \approx &-\frac{1}{4\pi\mu}\left\{\left[\left(1 + \frac{C_T^2}{C_L^2}\right)\ln r + \ln\frac{\omega}{2C_T} + \frac{C_T^2}{C_L^2}\ln\frac{\omega}{2C_L}\right]\delta_{kj}\right. \\ &\left. - \left(1 - \frac{C_T^2}{C_L^2}\right)r_{,k}r_{,j} + \mathrm{i}\frac{3\pi}{2}\left(1 + \frac{C_T^2}{C_L^2}\right)\right\}, \end{aligned}$$

$$(P^*_{kj})^{as} \approx -\frac{1}{2\pi r}\frac{C_T^2}{C_L^2}\left\{\left[\delta_{kj} - 2\left(1 - \frac{C_L^2}{C_T^2}\right)r_{,k}r_{,j}\right]\frac{\partial r}{\partial n} - [n_k r_{,j} - n_j r_{,k}]\right\}.$$